Dynamic contrast-enhanced MRI in cancer

Dynamic contrast-enhanced MRI has been proven to be a valuable technique in cancer imaging. The poorly formed and leaky vessels formed during angiogenesis to supply tumors facilitate an increased uptake of intravenously administered contrast agents in comparison to normal vasculature. The use of mathematical modeling techniques on the change in tumor signal intensity as a function of time provides a valuable insight into the underlying microvasculature of tumors. As an area of active research, the imaging and modeling of dynamic contrast-enhanced MRI data has many challenges. Novel contrast agents and models contribute to a refining of the technique and its application as a diagnostic tool in cancer imaging.

KEYWORDS: cancer ■ contrast agents ■ dynamic ■ MRI ■ pharmacokinetic modeling

Fiona J Gilbert[†]
& Trevor S Ahearn

[†]Author for correspondence:
Aberdeen Biomedical Imaging Center, Division of Applied Medicine, University of Aberdeen, Foresterhill, Aberdeen, AB25 2ZD, UK
Tel.: +44 122 455 9718;
Fax: +44 122 455 9718;
f.j.gilbert@abdn.ac.uk

In order for tumors to grow beyond a few millimeters in size new blood vessels are formed [1,2] to deliver metabolites and oxygen [3]. This angiogenesis is stimulated by a variety of factors partly from the tissue hypoxia in the center of the tumor and mainly from tumor–host interactions producing a variety of agents, the best known being VEGF. The vessels produced are different from those in normal tissue as they are heterogeneous with many distorted and twisting capillaries that have fragile walls. There are many arteriovenous shunts and areas of high vascular density that are interspaced with hypoxic areas [4]. VEGF is a glycoprotein that acts on tyrosine kinase receptors. The capillary walls are 'leaky' owing to widened endothelial fenestrae and an immature basement membrane. The binding of VEGF with endothelial cell receptors results in increased capillary permeability, allowing plasma proteins and activated endothelial cells to escape into the extracellular space. VEGF expression is positively correlated with microvessel density (MVD) [5]. Intravenous contrast has been used in MRI to great effect, allowing improved conspicuity of tumors, owing to the relative increase in vascularity found in many malignancies, such as breast, primary rectal and colorectal cancer, compared with normal tissues.

There are different categories of magnetic resonance (MR) contrast agent. These can be classified according to their features such as the type of their metal centers, their magnetic properties, chemical structure and biodistribution [6]. Those used in human dynamic contrast-enhanced (DCE)-MRI studies are typically extravascular and extracellular. These contrast agents are liquids that are injected intravenously, although they can be administered orally. The contrast agents most widely used in cancer imaging are gadolinium (Gd) based, intravenously administered and have a low molecular weight allowing easy passage into the extravascular space, particularly where vessels are leaky. The first of these to be approved for clinical use was Gd diethylene triamine pentaacetic acid (Gd-DTPA) [7]. These contrast agents do not cross cell membranes and remain in the extracellular space. The presence of the contrast agent shortens the longitudinal (T_1) and transverse (T_2) relaxation times of the surrounding tissue, which will increase the measured image signal on T_1-weighted imaging [8].

Different to the Gd-chelated contrast agents, nanoparticle-sized iron oxide contrast agents (i.e., ultra-small superparamagnetic iron oxide and superparamagnetic iron oxide, which are preferentially taken up by the reticuloendothelial system) have also been successfully used in MRI in cancer [9]. Their superparamagnetic property produces a very strong effect on transverse and apparent transverse relaxation rates (T_2 and T_2^*, respectively), where T_2^* is the combined effect of the actual transverse relaxation rate (T_2) and other field inhomogeneity effects. These contrast agents are the subject of much research. First used in liver imaging, they have more recently been used in lymphatic imaging. An orally administered manganese-based contrast agent has also been used in imaging liver cancer [10]. Although used in humans, these are discussed here for completeness, as the rest of this article is concerned with the application of Gd chelates in cancer.

part of
future medicine fsg

The ability to record contrast enhancement over a period of time has resulted in information becoming available regarding the state of the microvasculature of tissue. DCE-MRI requires sequential imaging over the same anatomical region before, during and after injection (or infusion) of a contrast agent. Simple workstation calculations of enhancement ratios and plotting of signal change over time have improved the specificity of the contrast-enhanced MRI examination, allowing differentiation of benign and malignant breast disease [11]. It has been recognized that analysis with sophisticated pharmacokinetic modeling can result in further useful information pertaining to the tumor, which can potentially be used as a biomarker to phenotype patients or as a treatment-response monitoring tool.

DCE-MRI technique

Unlike nuclear medicine techniques, where there is a direct detection of the tracer itself, and contrast computed tomography, where the contrast agent affects the attenuation of x-rays, the changes in the signal intensity on a contrast-enhanced MRI examination are a reflection of the effects of the contrast agent on hydrogen protons in tissue water. The vast majority of contrast-enhanced studies undertaken utilize chelated Gd ions as contrast agents, of which there are several commercially available variants [12]. These are small molecules (<1000 Da) and freely distribute through the extravascular extracellular space. They have relatively short biological half-lives (a few hours), clear by glomerular filtration and do not cross cell boundaries into the intracellular space owing to their size and hydrophilic nature. This characteristic behavior implies that there are two physiological compartments that Gd chelates can be found *in vivo*: the vascular compartment and the interstitial compartment.

As it is the modified relaxation of protons that is being detected in the dynamic experiment, the movement (exchange) of water molecules between tissue compartments becomes an important consideration in DCE imaging. Water exchange is accepted as being 'fast' across cell membranes. However, the exchange between vascular and extravascular space is considerably slower [13]. The rate of transcytolemmal water exchange (between vascular and interstitial space) is an area of current research. The effects of this exchange on DCE-MRI analysis have been investigated and shown to affect the accuracy of the quantitation of concentration of contrast media within tissue [14,15].

As they approach one another, the interaction between the unpaired electrons in the outer shell of the Gd ion and the nearby hydrogen proton causes a change in the nuclear magnetic relaxation rate of the proton [16]. This effect is highly dependant on the separation between the Gd and the proton and it is something of a compromise that the reduction in toxicity of nonchelated Gd is offset by a reduction in the overall effectiveness as a contrast agent. This is because the chelating agent, for example DTPA, provides a shell encasing the Gd ion, reducing the number of potential interaction sites and increasing the minimum separation distance with a hydrogen proton. The Solomon–Bloembergen–Morgan equation [17] can be used to describe the relaxivity effect of a paramagnetic contrast agent.

The presence of a Gd ion in a capillary causes a small magnetic field. This is due to the paramagnetic nature of Gd and its susceptibility to become magnetized in a magnetic field. This field gradient induces local magnetic field inhomogeneity, which extends for a few capillary diameters from the capillary itself, much greater than the nanometer range of the relaxivity effects. The effect of this additional gradient is much the same as any other field gradient in MRI in that there is a reduction in T_2^* in its vicinity. This magnetic susceptibility effect is in addition to the relaxivity effects discussed and these are the two completely different mechanisms by which MRI contrast agents function [18,19].

Since both T_1 and T_2^* are altered by the presence of contrast media, every DCE-MRI experiment will have a component of both processes. It has been suggested that for some studies preloading the tissue with a low dose of contrast media reduces the T_1 effects (T_1 shine through), which can contaminate T_2^* studies [20]. This contamination is due to the combination of T_1 shortening (signal increase) and T_2^* (signal decrease), which can result in inaccuracies in parameter estimation. The presence of a low concentration of contrast agent in the tissue reduces the relaxivity signal changes that are seen after additional doses of contrast. There is a concentration dependence of the dominant signal changing effect of the contrast agent: at low concentrations, the T_1 effect dominates and signal increases will be seen on T_1-weighted imaging. At higher doses, the T_2^* effect dominates and a signal drop will be observed on a T_2^*-weighted image. Clinically it is usual to use doses of 0.1 mmol/kg body mass, which equates to around 10–15 ml for an adult, although higher doses have been used. There have been

reports of nephrogenic systemic fibrosis linked to the use of high doses of Gd-based contrast agents in individuals with reduced renal function [21]. As such, these higher doses are less favored and renal function tests using estimated glomerular filtration rate are often performed before administration of MR contrast.

The choice of imaging sequence is used to maximize the effects of T_1 or T_2 relaxation. T_1-weighted studies are usually performed with short repetition time (TR) and echo time (TE) times using a FLASH sequence (known as T1-FFE on Philips and Spoiled GRASS on GE scanners). T_2^* imaging is achieved with long TR and TE times [22] often using echo planar imaging. Fat suppression may be implemented in order to improve visibility of enhancing regions [23,24].

The image acquisition methodology implemented in dynamic imaging of a lesion is dependant on the information that is required. Broadly, there are two image acquisition approaches. First, a relaxivity-based approach can be used to assess tumor microcirculation. Repeated T_1-weighted images are acquired and an increase in signal intensity is observed owing to the T_1-shortening effect of the contrast agent. Second, a susceptibility approach can be used to assess tumor perfusion. Here, rapid T_2^* imaging is performed and a signal drop is observed owing to the increased dephasing of spins in the presence of the small field gradients in the capillary bed. Dynamic T_2^* imaging has been predominantly used in neuroimaging. Here, the blood–brain barrier minimizes the leakage of the tracer and therefore eliminates any T_1 shine through. In regions where there is leakage of the tracer (e.g., where the blood–brain barrier is compromised) there will be leakage of contrast agent and quantitation of perfusion becomes more challenging. Figure 1 shows precontrast, postcontrast and difference images for a patient following two separate injections of Gd-DTPA and investigated using T_1- and T_2^*-weighted dynamic MRI. Figure 2 shows the resulting enhancement curves for the T_1- and T_2^*-weighted studies.

For T_2^*-weighted investigations, a bolus injection is necessary. However, injection protocols in T_1-weighted investigations vary. Some studies advocate bolus injection while others use a constant infusion. Bolus injections are commonly finished with a saline flush. Clearly the advantage of the bolus injection is the greater maximum plasma concentration and therefore tissue enhancement [25]. However, it has been
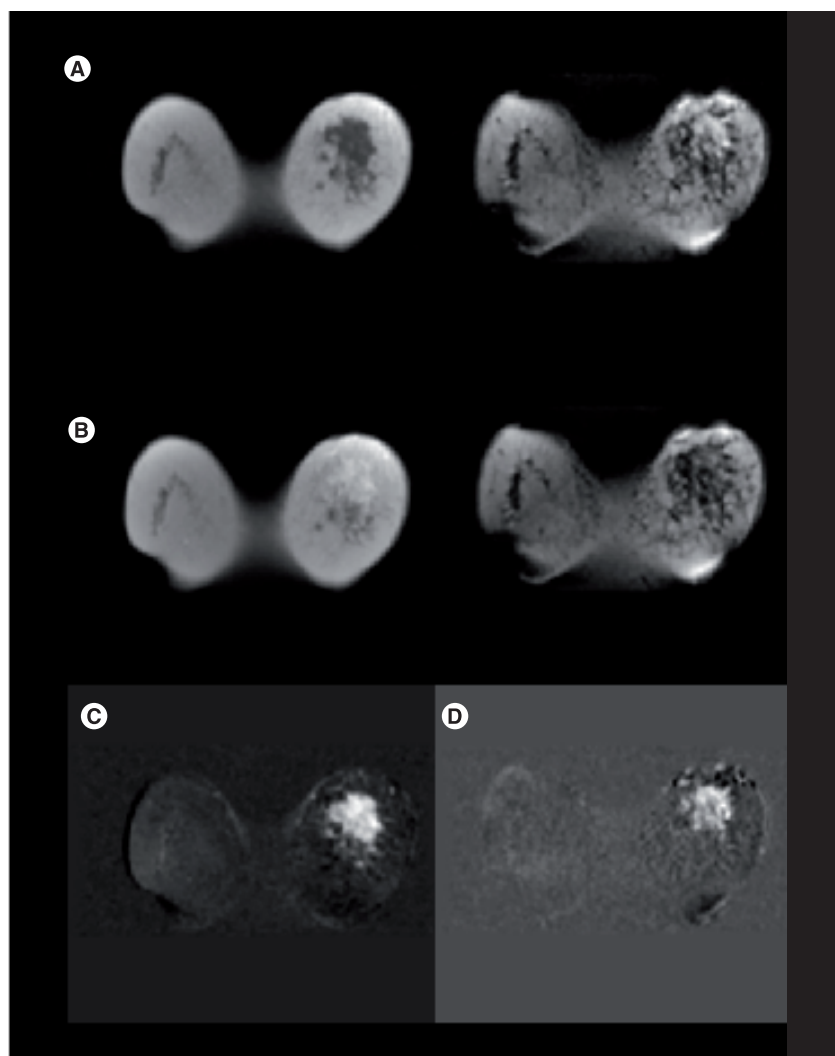

Figure 1. Breast images showing (A) precontrast, (B) postcontrast and (C & D) difference images acquired with separate bolus injections of Gd-DTPA and imaged with (C) T_1-weighted and (D) T_2^*-weighted sequences on a 1.5 T GE scanner.
Gd-DTPA: Gadolinium diethylene triamine pentaacetic acid.

suggested that constant-rate infusions allow for data acquisition with a longer temporal resolution where the rapid signal change due to a bolus may not be sampled adequately [26]. In either case, it is common to use a pump injector to ensure reproducible injection times of the viscous contrast medium.

In dynamic MRI, there is always a compromise between temporal and spatial resolution [27]. For a given spatial resolution there are a required number of phase-encoding steps. The greater the number of phase-encoding steps needed per time point, the longer it takes to acquire each set of data. Hence, less time points can be acquired over the duration of an imaging protocol. High spatial resolution allows better investigation into the heterogeneity of a tumor, while high temporal resolution allows more robust estimation
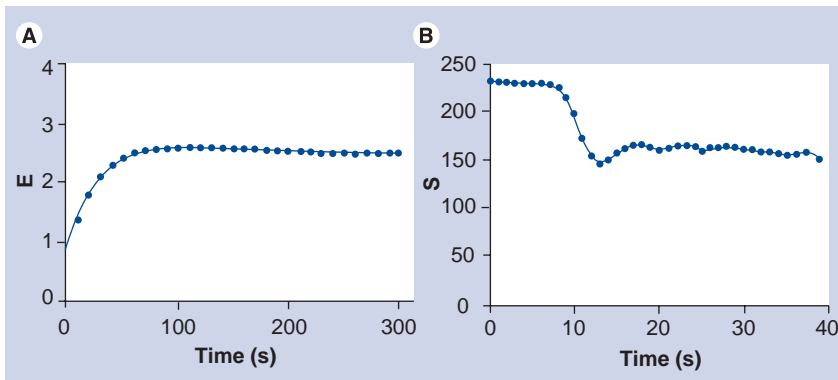
Figure 2. Dynamic uptake curves. (A) shows an example enhancement curve taken from a T_1-weighted study. Here, E represents the relative signal enhancement. **(B)** shows the signal changes resulting from the first pass of the bolus injection in a dynamic T_2^* study of the same individual.

of pharmacokinetic parameters. Suggestions for the minimum acceptable temporal resolution for pharmacokinetic modeling have been made [28]. T_2^* studies require resolutions of the order of a second to allow complete and accurate sampling of the first pass of the tracer. T_1 studies do not usually require the measurement of the first pass of the bolus since it can be modeled. Although, T_1 studies may require resolutions of 20 s or less to accurately sample the enhancement curve and ensure robust parameter estimation because of the presence of noise. Owing to these temporal sampling needs and given that T_2^* imaging requires a long TE to achieve sufficient T_2^* weighting, it is usual that there is less volume coverage in dynamic T_2^* imaging as very few slices can be acquired in the time available.

Improvement in scanner performance and the development of parallel imaging using techniques such as SENSE [29] and SMASH [30] has improved the quantity of data acquired in dynamic studies. Imaging using a combination of parallel imaging with/without selective k-space sampling techniques [31] allows a greater coverage. However, these technologies incorporate an inherent reduction in the signal-to-noise ratio of the acquired images owing to the reduced number of phase-encoding steps per image and need to be implemented with care [32].

Quantitation/analysis of signal change

Quantitation of the DCE-MRI signal change as a function of time has been and still is an active area of research. The manner in which DCE-MRI is approached can be broken into different levels of complexity. The simplest method of interpreting DCE data is purely qualitatively, in other words, no measurements are made on the images, they are used to observe

areas that show marked signal change. A more complex approach is a semiquantitative analysis of the plots of signal intensity versus time. These plots can then be categorized according to their shape [33] and have been used to differentiate benign from malignant tumors. FIGURE 3 shows an example classification scheme as used in the Magnetic Resonance Imaging for Breast Screening (MARIBS) trial [34].

Simple image analysis methods that utilize user-defined regions of interest (ROI) over the whole tumor are available on many clinical workstations. However, these methods do not provide the facility to investigate the heterogeneity often found in tumors. In addition, user-defined ROIs make use of DCE-MRI in treatment monitoring difficult owing to inter- and intraobserver variability and the difficulty in accurate ROI placement between imaging sessions. Analysis of DCE-MRI data is more commonly performed on a pixel-wise basis. Here, parametric maps of a tumor can be produced and tumor heterogeneity visualized. FIGURE 4 shows a parametric map of a breast tumor overlayed onto an anatomical image. Signal enhancement or parameter 'hot spots' and histograms of enhancement parameters have been used in attempts to improve the specificity and simplify the pixel-wise analysis of tumor enhancement [35] in treatment monitoring.

By normalizing the signal-versus-time curve to the baseline signal, level enhancement curves for a tumor can be generated. From these curves enhancement ratios can be calculated using a variety of metrics [36,37]. These semiquantitative measures of enhancement provide useful but flawed assessment of enhancement. These methods fail to account for the dependence of signal change on the precontrast properties of the tissue or the imaging sequence used. Furthermore, semiquantitative measurements not incorporating a measurement of the time-to-signal peak (or similar) may fail to account for the effect of cardiac function and delivery of the contrast agent to the tissue [38].

Pharmacokinetic analysis (pharmacokinetic/compartmental modeling) describes the process whereby mathematical models, which describe the underlying physiology of tissue, are fit to signal enhancement data. These models attempt to quantify properties of tumor tissue that are independent of scanner or acquisition protocol. Data are fitted to the model using one of a number of optimization or curve-fitting techniques. The two most popular algorithms are the Levenberg–Marquardt [39] and simplex minimization [40] algorithm. These algorithms perform the data

fit by minimizing the sum of the squares of the differences between the data collected and the model estimated time curve. In either case it is often necessary to adjust settings within the algorithm in order to achieve the correct fit [41], hence some vigilance is required in interpreting results.

The pharmacokinetics of tracer distribution and passage has been of scientific interest since the early 20th century when researchers were investigating blood flow through organs using indicator dilution theory. This provided the mechanism to relate an infused mass of a contrast agent or tracer (the indicator), organ blood flow rate, distribution volume and the time taken for the tracer to traverse the organ (the transit time). The organ (or body) is described as a compartment (or series of compartments) that the contrast agent travels through. Inside the compartment the contrast agent is assumed to be evenly and instantly distributed, the passage between the compartments is based on Fick's law, which states that the rate of exchange of contrast agent between compartments is proportional to the difference in contrast agent concentration between them.

In describing models for T_1-weighted DCE-MRI, flow- and permeability-limited uptake must be considered. In tissues where there is a reduction in perfusion, such as large tumors with necrotic centers, measurements of contrast agent leakage may be flow limited. Here, highly leaky vasculature will only demonstrate leakage in proportion to the locally supplied dose, and perfusion rather than capillary permeability will be the determinant of enhancement. By comparison, when flow is high and permeability is low then the uptake will be permeability limited. Models describing limited uptake cases are described in the literature [42].

Relaxivity studies (T_1-weighted DCE MRI) commonly use models that fit for free parameters describing leakage or interstitial space (v_e), permeability surface area product or transfer constant (K^{trans}) and the efflux constant K_{ep} (numerically equivalent to K^{trans}/v_e). Susceptibility studies (T_2^* weighted) fit for regional blood volume, regional blood flow and mean transit time, although there is some debate as to the precise definition of mean transit time [43].

Mathematical models of varying degrees of complexity can be constructed in attempts to correctly model the underlying tissue microvasculature. However, the more complex the model the greater the number of free parameters required in the fit. This has a direct impact on the robustness of the fitting process due to the
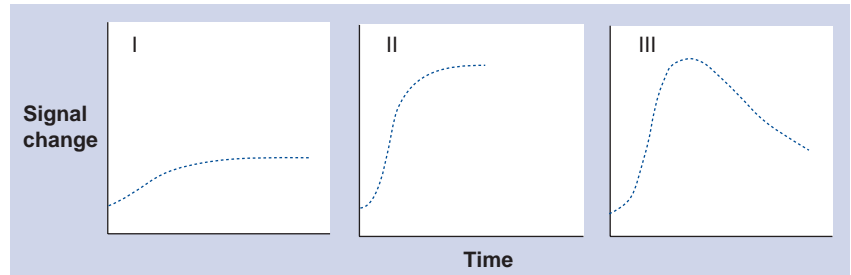

Figure 3. Enhancement curve classification scheme as used in the Magnetic Resonance Imaging for Breast Screening trial.

interactions between parameters on the shape of the curve. There are a number of pharmacokinetic approaches in the literature of varying complexity [44–50]. The simplest model fits two parameters to the contrast agent concentration curve. This approach is used the most and is described by Tofts [45]. A schematic of this model is shown in FIGURE 5. The more complicated models have more fitted parameters but they all require the MRI signal to be converted to the concentration of tracer for parameter fitting. This is usually done by assuming that the change in proton relaxivity rate is proportional to the concentration of tracer with the constant of proportionality being the measure of the tracer's effectiveness as a MRI contrast agent.
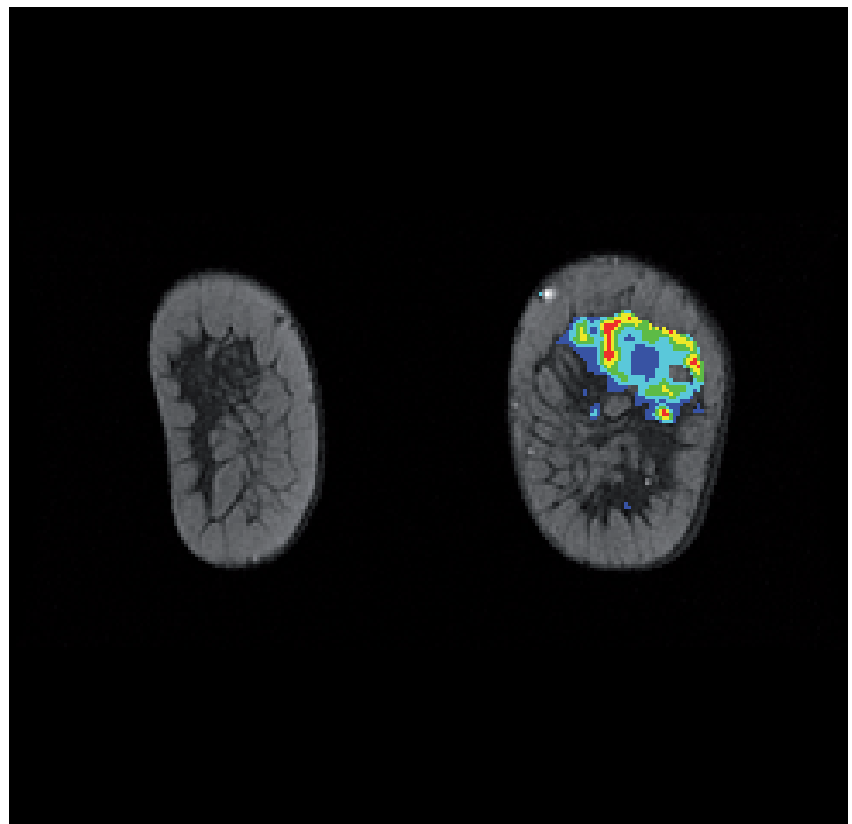

Figure 4. Image showing a pharmacokinetic parameter map overlayed onto a structural MRI. Here, red and yellow pixels represent rapidly enhancing regions.
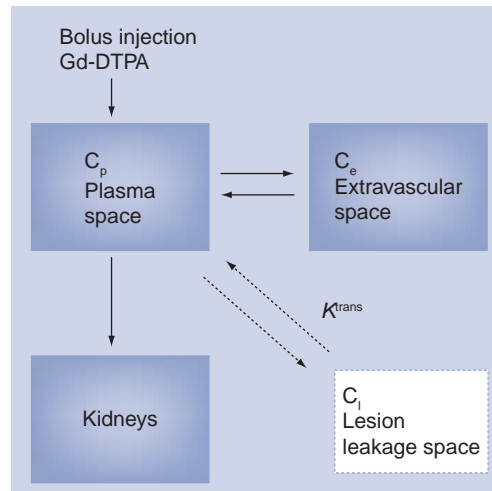
Figure 5. Tofts' compartment model describing the distribution of an extravascular contrast agent. Here, K^{trans} represents the transfer rate between the plasma and lesion compartments. C_l, C_p and C_e represent the concentrations of contrast agent within each compartment.
Note: C_e is the concentration of contrast agent within the extravascular compartment. C_l is the concentration of contrast agent within the lesion compartment. C_p is the concentration of contrast agent within the plasma compartment. Gd-DTPA: Gadolinium diethylene triamine pentaacetic acid.

The majority of these models are measuring the same physiological features and, as such, a standardization of the language used in DCE-MRI has been proposed [42]. Despite their added complexity, it has been suggested that simple quantitative approaches are numerically correlated with pharmacokinetic parameters [51].

Pharmacokinetic models have been extended to incorporate an assessment of the input function and account for the delivery characteristics of the contrast agent. Input functions that are assumed to be constant for all investigation [7,45], simplify the analysis but introduce a significant source of error from the normal variation in renal clearance of contrast agent from the plasma [52]. These errors can be avoided with input functions that are specific to each study. The input function is calculated from a suitable blood vessel in the imaging field. However, it is sometimes difficult to find suitable vessels within the image field of view so this has encouraged the use of more esoteric methods to quantify an input function. Researchers have used literature values for permeability and leakage volume of reference tissues (muscle and white matter) [53–55] in a way to impute a suitable arterial input function (AIF). Voxel-specific AIF has been demonstrated in the brain using a computerized detection of voxels with the earliest and largest signal decay (representing blood vessels) and this approach is made more sophisticated by also accounting for the dispersion and delay of contrast delivery. This is in an attempt to relate an area of tissue enhancement to a more local blood vessel and therefore a more relevant input function [56] but this has yet to be applied in noncranial imaging. Population-averaged AIFs have been developed and applied in a patient cohort [57,58] and have been shown to improve the reproducibility of tracer kinetic modeling. Furthermore, the incorporation of cardiac output (measured using phase-contrast MRI) has been proposed to give additional reproducibility [58].

As already mentioned, measurement of the native (precontrast) T_1 is required to convert the measured signal enhancement time course data into the contrast concentration time course data. Direct use of signal change cannot be used for accurate quantitation of enhancement owing to the dependence of enhancement on precontrast T_1. This causes tissues with a long inherent T_1 to display a greater signal change per unit concentration of contrast media than those with short T_1. During dynamic investigations T_1 is usually measured using multiple flip angle FLASH acquisitions, as the long acquisitions required for inversion recovery methods makes them unattractive clinically. The short TR used in T_1-weighted FLASH (required for sufficient T_1 weighting) has recently been shown to produce significant errors in T_1 calculation owing to incomplete spoiling of magnetization [59]. This has a follow on effect on enhancement measurement [60,61]. These errors in T_1 could possibly be corrected by calibration using appropriate phantoms since the magnitude of the T_1 error will be constant for a given T_1 and TR.

Additional complications in T_1 estimation are present in 2D imaging. Here, slice profile effects need to be considered in the calculation of T_1 as the shaped pulses radiofrequency that produce the MRI signals also result in nonrectangular slice profiles [62]. Owing to their broad profile, 3D acquisitions have rectangular slice profiles through the center of the slab and are only affected by profile effects at the edges of the 3D slab. Further consideration in calculation of native T_1 is the homogeneity of the B_1 field. Using surface coils there is the potential for significant flip angle inhomogeneity across the field of view. This directly affects the robustness of T_1 calculation [63] and, hence, enhancement measurement and pharmacokinetic parameter estimation. This is a greater problem at higher field strengths (3 T) [64].

Use of DCE-MRI in breast cancer

Dynamic contrast-enhanced MRI has been used as a method to improve diagnostic specificity and to better characterize lesions noninvasively. This has been widely used in breast imaging. Commercial workstations provide a variety of simple analysis tools to make measurements such as signal enhancement ratio (SER), maximum slope of enhancement, time to peak enhancement (TPE) and maximum enhancement.

Malignant tumors tend to enhance more strongly than benign lesions [65] and this enhancement tends to occur earlier than that of benign lesions [66]. Quantification of the initial uptake slope has been documented [67,68] as well as the percentage enhancement [69]. The TPE is the time taken for the signal to peak following contrast injection. This has been shown to be useful in differentiating malignant lesions. Gilles showed that a larger number of malignant lesions enhanced 47 s after contrast than benign lesions of which the majority showed enhancement at 94 s [70]. However, with very rapid image acquisition, for example every 9 s, the peak tends to occur at 20–30 s.

It has become clear that tumors are very heterogeneous with some showing a slow increase in signal over time with a fairly homogenous enhancement pattern whereas others can demonstrate a rim enhancement specific to malignancy with a rapid rise in signal with an early peak and a washout pattern, typical of malignancy. These dynamic signal intensity time courses have been described as type 1 – a slow continuously increasing signal over time, most commonly characterizing benign lesions, type 2 – rapid rise over 1–2 min with a plateau, a pattern that is indeterminate for malignancy, and type 3 – rapid rise in signal reaching a peak within 1–2 min and then washing out by more than 10%, a pattern considered typical of malignancy. In a series of 266 breast lesions, Kuhl found the probability of malignancy with a type 1 curve was 8.9%, type 2 curve 33.6% and with a type 3 curve 57.4% [11]. This information had much improved specificity compared with using only enhancement rates in the first minute (83% compared with 37%).

There has been much debate over whether or not more rapid temporal acquisition with reduced spatial resolution has a detrimental effect on diagnostic accuracy. In a comparison of 30 patients with 54 breast lesions, Kuhl demonstrated that the increased spatial resolution that could be achieved by imaging every 118 s compared with every 69 s resulted in improved assessment of morphological criteria. While there was some loss of differentiation of benign and malignant lesions using the early enhancement ratios, the overall shape of the time curves were unaffected [27]. In a study to estimate the contribution of the DCE component to diagnostic accuracy, Warren examined breast lesions from the MARIBS trial of women at high risk of developing breast cancer and showed that the morphological features were more important in determining whether a lesion was benign or malignant [71]. This supports the high spatial resolution technique that has been largely adopted in Europe with breast imaging taking up to 2 min for each time point in the dynamic acquisition.

No gold standard exists to measure tumor physiology and verify the pharmacokinetic measurements obtained with this technique [15]. The value of this technique will be defined by the clinical utility [72]. Most studies have compared pharmacokinetic parameters with clinical outcome or have used histopathology with tumor grade, lymph node status, tumor size, MVD or VEGF expression in correlative studies of prognostic factors. The slope of the enhancement curve is associated with MVD [73] and it was shown that nodal status of a breast tumor and histological grade were strongly associated with enhancement characteristics [74]. In response-monitoring studies, objective measures of tumor response such as changes in tumor size or volume are used as the the end point.

Response biomarkers are used to monitor the effects of neo-adjuvant chemotherapy. In breast cancer, MRI has been widely investigated and shown to be superior to conventional imaging techniques of mammography and ultrasound in measuring changes in tumor size – the traditional assessment of response. There is a considerable body of literature reporting the use of MRI for monitoring neo-adjuvant chemotherapy in women with locally advanced breast cancer. However, most studies are small, with variable techniques and inconsistent end points making it difficult to assess the value or reproducibility of this and the value to the clinician in patient management. There is agreement that MRI is superior to clinical examination, mammography and ultrasound in assessing disease extent on completion of chemotherapy in order to plan surgery [75,76], although this technique cannot detect small residual foci of viable tumor cells. The Blue Cross Shield review included 18 studies and showed that MRI consistently had a sensitivity of 90–100% and specificity of 50–100% in detecting residual disease using histopathology as the gold standard [77]. In five of the studies

the actual size and disease extent was compared with final histopathology and the accuracy varied between 57 and 97% with correlation coefficient of 0.72–0.98.

Studies in breast cancer have been undertaken to ascertain whether any of the baseline MRI parameters could be used to predict response to treatment but so far none have found them to be useful. A reliable assessment of lack of response would allow the oncologist to switch to a more effective chemotherapy regime earlier in patient management. However, there is a study in renal cancer where MRI parameters were able to predict response [78].

Several studies have shown a reduction of the tumor vascularity, as measured by slower and lower contrast enhancement, to precede a reduction in measurable tumor volume. The Blue Cross Shield review of six breast studies assessing the value of MRI in monitoring treatment found results to be inconsistent, with low patient numbers and only two of the studies reporting a negative predictive value of 58 and 83% in identifying those patients who were not responding to chemotherapy [79]. Some of the patients who did not show any response after two courses of treatment went on to have at least a partial response.

Both K^{trans} and v_e have been used to assess response to chemotherapy. K^{trans} is promising and reduction by more than 50% has been linked to response to treatment (evaluated by core biopsy) in breast cancer [35,80,81]. The peak amplitude v_e has also been shown to be useful with a reduction in the peak corresponding to response [82]. However, the combination in changes in volume with changes in enhancement ratio increases the specificity of the detection of patients who will achieve a complete pathologic response [83,84]. In a study of 68 patients it was found that both K^{trans} and K_{ep} were significantly reduced (p < 0.001) in eventual responders at a median of 54 days following treatment. They also found that v_e increased significantly in the nonresponders. Similarly, Padhani found that K^{trans} increased in nonresponders after one cycle of treatment and found K^{trans} reduced significantly in responders after two courses of chemotherapy, although changes were not significant after only one course of treatment [85].

However, not all groups have concluded that pharmacokinetic parameters are of value. In a series of 29 patients, Yu found that after one course of chemotherapy tumor volume was a better predictor of response compared with pharmacokinetic measurements [86]. Manton's

group found no correlation between pharmacokinetic parameters after two cycles of treatment and response measured from eventual tumor volume [87].

Correlative studies have demonstrated the potential of DCE-MRI as an imaging biomarker in terms of proof of concept. However, large-scale multicenter studies are required to demonstrate reproducibility across sites, and to test standardized protocols for data acquisition and marker quantification [72].

DCE-MRI in cervical cancer

A robust assessment of therapy response would be very helpful in the management of locally advanced cervical cancer where the standard therapy regime consists of concurrent chemotherapy and radiotherapy (chemoradiation). The addition of chemotherapy to the radiotherapy regime has been shown to improve survival [88–91], although there are increased complications and morbidity [91].

Noncontrast MRI is the most reliable imaging method for staging and planning therapy for cervical cancer [92]. DCE-MRI has been used as a useful prognostic indicator in cervical carcinoma treated with radiotherapy [93], particularly when combined with an assessment of morphology [94]. Initial attempts to stage locally advanced cervical cancer using DCE-MRI with pharmacokinetic analysis demonstrated that standard radiological assessment of T_2-weighted MR data was superior to pharmacokinetic analysis [95]. However, another group demonstrated that pharmacokinetic analysis of pretherapy DCE-MRI data reflects tumor oxygenation and showed promising prognostic information of patient survival [96]. The potential for DCE-MRI pharmacokinetic analysis to predict radiotherapy response in a small cervical cancer group has been demonstrated [97]. Our own group, using previously validated in-house software [41,98,99] to undertake pharmacokinetic modeling of dynamic data, showed that baseline K^{trans} was significantly correlated with clinical response, and remained significantly associated with clinical response when combined with v_e (predicting over 65% of the variance of clinical response). Using workstation parameters (Functool, GE, Waukesha, WI, USA) in the same group of patients, the maximum slope of increase, TPE and SER were calculated. Pretherapy maximum slope of increase, TPE and SER individually correlated with eventual clinical response. Using these two approaches and combining the results in a univariate model, we were able to predict over 88% of the variance of

clinical response in a single 30-min DCE-MRI examination pretherapy. Individually, a radiological assessment of DCE-MRI pretherapy data is predictive of locally advanced cervical cancer response to chemoradiotherapy, as is a pharmacokinetic assessment; however, the combination of these assessments improves the predictive power by over 20% [100].

DCE-MRI in colorectal cancers

Although histological assessments of MVD have been used with variable success to predict grade, metastatic potential and response to therapy, the technique of histological assessment is difficult to reproduce robustly. However, bevacizumab (Avastin, Genentech), in addition to conventional chemotherapy, has been successfully shown to improve survival in patients with colorectal metastases [101,102], suggesting that the function of the microvessel is an important factor. Qualitative T_1-based DCE-MRI measurements such as slope of enhancement and maximal enhancement have been shown to correlate with grade of the rectal cancer and MVD [103]. Correlations have been found between serum VEGF and K^{trans} [104].

A combination of chemotherapy and radiation is used to treat primary rectal cancers. Ionizing radiation causes upregulation of VEGF in cancer cell lines either as a direct effect or through endothelial hypoxia inducible factor activation [105]. In one study of 11 patients, the mean perfusion index increased in the first 2 weeks following chemoradiation but decreased by week 4 (although values were still above the baseline measurements) [106]. It has been shown that a decrease in K^{trans} follows successful treatment [104]. Higher baseline K^{trans} can predict poorer response to chemoradiation [107] but the opposite was found by George *et al.* [104]. These studies are small and further work needs to be done in this area.

Pharmacodynamic biomarkers in Phase I & II drug studies

The advent of anti-angiogenic drugs has resulted in the investigation of DCE-MRI as a predictive biomarker. Several Phase I studies of anti-angiogenic therapies have used DCE-MRI in the assessment of efficacy with variable results. Bevacizumab is an anti-VEGF agent that has been successfully used clinically in tumors with high VEGF levels [108,109]. In a pilot study of locally advanced breast cancer, patients were given bevacizumab alone for the first cycle and then in combination with conventional chemotherapy. The pharmacokinetic parameters of

K^{trans}, K_{ep} and v_e all reduced after the single agent bevacizumab and continued to decrease with subsequent cycles but these could not be used to differentiate responders and nonresponders [110]. In a Phase II trial of bevacizumab given 3 days before conventional chemotherapy for six patients with osteosarcoma, K^{trans} and v_e did not change substantially but K_{ep} was found to decrease over the course of treatment [111].

In a Phase I study of valatinib, which inhibits multiple VEGF receptors, DCE-MRI of hepatic metastases was undertaken in 26 patients. Here, measurements of the transfer constant was found to be negatively correlated with oral dose and plasma levels of the experimental drug with significantly greater reduction in the transfer constant in those patients who did not have progressive disease [112]. However, the Phase I MR findings did not predict a successful outcome for the Phase III trials in combination with FOLFOX [102].

In Phase I studies, traditionally drug toxicity has been used to inform dose schedules for further investigation. However, anti-angiogenic drugs are relatively well tolerated and have a wide therapeutic window so DCE-MRI can be used to define the biologically active dose.

Recommendations from the UK workshop on use of MRI in antivascular & anti-angiogenic therapies

The purpose of this workshop was to produce guidance for investigators designing trials of novel agents where DCE-MRI was being incorporated to assess drug activity. The group stated that "The main interest in functional imaging end points are in Phase I/II trials with the objectives of obtaining an accurate marker of biological efficacy, identifying the biologically effective dose … and evaluating scheduling options and possible combination therapies" [113]. The techniques are required to be acceptable to patients, feasible, reproducible, applicable to multiple centers, and must be implemented in a standardized way across centers with prospective end point validation. The recommendations were that pharmacokinetic assessment [114] should use T_1-weighted studies of low-molecular-weight Gd chelates, and that T_2^*-weighted studies may provide further information. A measurement of K^{trans} (min^{-1}) or the initial area under the gadolinium curve (IAUGC) should be the primary end point. This requires that the precontrast tissue T_1 is calculated, cardiac output or an AIF is measured, a power injector is used and that the MR field is homogeneous. Contrast-enhanced tumor

voxels can be summed to give a volume and tumor volume should be measured. 3D measurements are preferred. Data sets with acquisition parameters and end points should be made available to allow different groups to develop analysis tools. This UK recommendation has not been widely adopted as yet. The NIH has promoted the formation of the Quantitative Imaging Biomarker Alliance (QIBA) [201]. One strand of this work is in DCE-MRI where it is hoped that acquisition and analysis standards will be agreed [202].

Conclusion

Dynamic contrast-enhanced MRI has been adopted in routine practice in the diagnosis of breast tumors. It is slowly being used in the diagnosis of other tumor types. The functional nature of DCE-MRI has been recognized as an important biomarker in the prediction and monitoring response in a variety of tumors. This is of particular relevance as anti-angiogenic drugs are used alone or in combination chemotherapy regimes. However, the importance of standardization of both acquisition techniques and analysis tools cannot be over emphasized if this valuable functional technique is to be widely adopted in clinical practice.

Future perspective

There is continued development of new contrast agents with different properties and molecular weights [6]. The development of macromolecular contrast agents will aid the investigation of tumor microvasculature owing to the reduction in their leakage into the extravascular space compared with small DTPA ligands. The macromolecular agent albumin Gd-DTPA has been used in imaging animal models of cancer [115] but is unfavorable for use in humans owing to incomplete clearance and potential immunogenicity [116,117]. Hence, other molecules are being investigated. Macromolecules structured around polyethelyne glycol are being developed for clinical use but have so far only been used in animal imaging [118]. Recent macromolecular contrast agent developments have been more thoroughly reviewed elsewhere [119,120]. Despite the potential for macromolecular contrast agents in imaging their clinical use can only progress once their safety is proven.

Nanoparticle contrast agents are also being developed [9] with particular effort being put into producing contrast media with a stronger T_1 effect than the current nanoparticle contrast agents. As with macromolecular development,

Executive summary

Dynamic contrast-enhanced MRI technique
- Dynamic contrast-enhanced (DCE) MRI is the sequential MRI of a tumor before, during and after intravenous administration of a contrast agent.
- The poorly formed neovasculature supplying tumors has a higher leakage of contrast media than normal vasculature.

Quantitation/analysis of signal change
- Quantitation can be performed at a range of complexity from enhancement ratios to sophisticated pharmacokinetic models.
- Pharmacokinetic models can be fitted to dynamic data to make measurements of the tumor microvasculature.
- MRI contrast agents can be used to measure tumor perfusion using T_2*-weighted imaging or tumor permeability using T_1-weighted imaging.

Use of DCE-MRI in breast cancer
- The specificity and sensitivity of cancer imaging is improved with the use of DCE-MRI techniques.
- Debate continues as to the trade-off between temporal and spatial resolution.

DCE-MRI in cervical cancer
- A robust predictor of therapy response would be very helpful in the management of locally advanced cervical cancer.
- The potential for DCE-MRI pharmacokinetic analysis to predict radiotherapy response in a small cervical cancer group has been demonstrated.

DCE-MRI in colorectal cancers
- Histological assessments of microvessel density have been used with variable success to predict grade, metastatic potential and response to therapy.
- Histological assessment is difficult to reproduce robustly.
- Qualitative T_1 measurements such as slope of enhancement and maximal enhancement have been shown to correlate with grade of the rectal cancer and microvessel density.

Predictive response in Phase I & II drug studies
- The advent of anti-angiogenic drugs has resulted in the investigation of DCE-MRI as a predictive biomarker.

Recommendations from the UK workshop on use of MRI in antivascular & anti-angiogenic therapies
- The recommendations were that pharmacokinetic assessment should use T_1-weighted studies of low-molecular-weight gadolinium chelates and that T_2*-weighted studies may provide further information. K^{trans} (min^{-1}) or area under the curve measurement should be the primary end point.

these new molecules need to be thoroughly tested for toxicological effects and long-term stability.

Developments in tissue targeting with labeled monoclonal antibodies would facilitate a directed noninvasive metric of angiogenesis. Recently, tagging of cells with Gd-based contrast agents has been demonstrated [121] and researchers have extended modeling for use with targeted contrast agents [122]. Vessel size imaging is a recent development presented in the literature. The extension of this into human cancers using differences in signal change after Gd injection between T_2-weighted spin echo and T_2*-weighted gradient echo imaging may provide valuable insights into tumor growth and therapy response [123]. It has been known for some time that there is a raised interstitial pressure within tumors. This may be a factor in chemotherapy response as this increased internal pressure will hinder delivery of drug therapy. The facility to image interstitial pressure with MRI is appealing and has been demonstrated in lung tumors [124].

Financial & competing interests disclosure

The authors have no relevant affiliations or financial involvement with any organization or entity with a financial interest in or financial conflict with the subject matter or materials discussed in the manuscript. This includes employment, consultancies, honoraria, stock ownership or options, expert testimony, grants or patents received or pending, or royalties.

No writing assistance was utilized in the production of this manuscript.

Bibliography

Papers of special note have been highlighted as:
- ▪ of interest
- ▪▪ of considerable interest

1 Folkman J: Tumor angiogenesis: therapeutic implications. *N. Engl. J. Med.* 285(21), 1182–1186 (1971).

2 Weidner N, Folkman J: Tumoral vascularity as a prognostic factor in cancer. *Important Adv. Oncol.* 167–190 (1996).

3 Carmeliet P, Jain RK: Angiogenesis in cancer and other diseases. *Nature* 407(6801), 249–257 (2000).

4 Knopp MV, Weiss E, Sinn HP *et al.*: Pathophysiologic basis of contrast enhancement in breast tumors. *J. Magn. Reson. Imaging* 10(3), 260–266 (1999).

5 Toi M, Inada K, Suzuki H, Tominaga T: Tumor angiogenesis in breast cancer: its importance as a prognostic indicator and the association with vascular endothelial growth factor expression. *Breast Cancer Res. Treat.* 36(2), 193–204 (1995).

6 Geraldes CF, Laurent S: Classification and basic properties of contrast agents for magnetic resonance imaging. *Contrast Media Mol. Imaging* 4(1), 1–23 (2009).

▪▪ **Detailed discussion of the various contrast agents in development.**

7 Weinmann HJ, Brasch RC, Press WR, Wesbey GE: Characteristics of gadolinium–DTPA complex: a potential NMR contrast agent. *Am. J. Roentgenol.* 142(3), 619–624 (1984).

8 Kenney PJ, Sobol WT, Smith JK, Morgan DE: Computed model of gadolinium enhanced MRI of breast disease. *Eur. J. Radiol.* 24(2), 109–119 (1997).

9 Na HB, Song IC, Hyeon T: Inorganic nanoparticles for MRI contrast agents. *Adv. Mater.* 21, 2133–2148 (2009).

10 Thomsen HS, Barentsz JO, Burcharth F *et al.*: Initial clinical experience with oral manganese (CMC-001) for liver MR imaging. *Eur. Radiol.* 17(1), 273–278 (2007).

11 Kuhl CK, Mielcareck P, Klaschik S *et al.*: Dynamic breast MR imaging: are signal intensity time course data useful for differential diagnosis of enhancing lesions? *Radiology* 211(1), 101–110 (1999).

12 Mitchell DG: MRI contrast agents – what's in a name? *J. Magn. Reson. Imaging* 7(1), 1–4 (1997).

13 Donahue KM, Burstein D, Manning WJ, Gray ML: Studies of Gd-DTPA relaxivity and proton exchange rates in tissue. *Magn. Reson. Med.* 32(1), 66–76 (1994).

14 Yankeelov TE, Rooney WD, Li X, Springer CS Jr: Variation of the relaxographic "shutter-speed" for transcytolemmal water exchange affects the CR bolus-tracking curve shape. *Magn. Reson. Med.* 50(6), 1151–1169 (2003).

▪ **Discusses water movement and its effect on modeling.**

15 Buckley DL: Transcytolemmal water exchange and its affect on the determination of contrast agent concentration *in vivo*. *Magn. Reson. Med.* 47(2), 420–424 (2002).

16 Lauffer RB: Paramagnetic metal complexes as water proton relaxation agents for nmr imaging: theory and design. *Chem. Rev.* 87, 901–927 (1987).

17 Bloembergen N, Morgan L: Proton relaxation times in paramagnetic solutions. Effects of electron spin relaxation. *J. Chem. Phys.* 34, 842 (1961).

18 Runge VM, Nelson KL: Contrast agents. In: *Magnetic Resonance Imaging (3rd Edition).* Stark DD, Bradley WG Jr (Eds). Mosby, Inc., USA 257–275 (1999).

19 Roberts TPL, Noseworthy MD: Contrast agents for magnetic resonance imaging. In: *Dynamic Contrast Enhanced Magnetic Resonance Imaging in Oncology.* Jackson A, Bucklay DL, Parker GJM (Eds). Springer-Verlag, Germany 23–37 (2003).

20 Kassner A, Annesley DJ, Zhu XP *et al.*: Abnormalities of the contrast re-circulation phase in cerebral tumors demonstrated using dynamic susceptibility contrast-enhanced imaging: a possible marker of vascular tortuosity. *J. Magn. Reson. Imaging* 11(2), 103–113 (2000).

21 Collidge TA, Thomson PC, Mark PB *et al.*: Gadolinium-enhanced MRI and nephrogenic systemic fibrosis: retrospective study of a renal replacement therapy cohort. *Radiology* 245(1), 168–175 (2007).

▪▪ **Emerging safety issue in contrast-enhanced imaging.**

22 Hendrick RE, Haacke EM: Basic physics of MR contrast agents and maximization of image contrast. *J. Magn. Reson. Imaging* 3(1), 137–148 (1993).

23 Ma J, Vu AT, Son JB, Choi H, Hazle JD: Fat-suppressed three-dimensional dual echo Dixon technique for contrast agent enhanced MRI. *J. Magn. Reson. Imaging* 23(1), 36–41 (2006).

24 Niitsu M, Tohno E, Itai Y: Fat suppression strategies in enhanced MRI of the breast: comparison of SPIR and water excitation sequences. *J. Magn. Reson. Imaging* 18(3), 310–314 (2003).

25 Tofts PS, Berkowitz BA: Measurement of capillary permeability from the Gd enhancement curve: a comparison of bolus and constant infusion injection methods. *Magn. Reson. Imaging* 12(1), 81–91 (1994).

26 Hoffmann U, Brix G, Knopp MV, Hess T, Lorenz WJ: Pharmacokinetic mapping of the breast: a new method for dynamic MR mammography. *Magn. Reson. Med.* 33(4), 506–514 (1995).

27 Kuhl CK, Schild HH, Morakkabati N: Dynamic bilateral contrast-enhanced MRI of the breast: trade-off between spatial and temporal resolution. *Radiology* 236(3), 789–800 (2005).

28 Henderson E, Rutt BK, Lee TY: Temporal sampling requirements for the tracer kinetics modeling of breast disease. *Magn. Reson. Imaging* 16(9), 1057–1073 (1998).

29 Pruessmann KP, Weiger M, Scheidegger MB, Boesiger P: SENSE: sensitivity encoding for fast MRI. *Magn. Reson. Med.* 42(5), 952–962 (1999).

30 Sodickson DK, Manning WJ: Simultaneous acquisition of spatial harmonics (SMASH), fast imaging with radiofrequency coil arrays. *Magn. Reson. Med.* 38(4), 591–603 (1997).

31 van Vaals JJ, Brummer ME, Dixon WT *et al.*: "Keyhole" method for accelerating imaging of contrast agent uptake. *J. Magn. Reson. Imaging* 3(4), 671–675 (1993).

32 Bishop JE, Santyr GE, Kelcz F, Plewes DB: Limitations of the keyhole technique for quantitative dynamic contrast-enhanced breast MRI. *J. Magn. Reson. Imaging* 7(4), 716–723 (1997).

33 Daniel B, Yen Y, Glover G *et al.*: Breast disease: dynamic spiral MR imaging. *Radiology* 209, 499–509 (1998).

34 Brown J, Buckley D, Coulthard A *et al.*: Magnetic resonance imaging screening in women at genetic risk of breast cancer: imaging and analysis protocol for the UK multicenter study. UK MRI Breast Screening Study Advisory Group. *Magn. Reson. Imaging* 18(7), 765–776 (2000).

35 Hayes C, Padhani AR, Leach MO: Assessing changes in tumor vascular function using dynamic contrast-enhanced magnetic resonance imaging. *NMR Biomed.* 15(2), 154–163 (2002).

36 Warren RM, Pointon L, Thompson D *et al.*: UK Magnetic resonance imaging in Breast Screening (MARIBS) Study Group. Reading protocol for dynamic contrast-enhanced MR images of the breast: sensitivity and specificity analysis. *Radiology* 236(3), 779–788 (2005).

37 Parker GJ, Suckling J, Tanner SF *et al.*: Probing tumor microvascularity by measurement, analysis and display of contrast agent uptake kinetics. *J. Magn. Reson. Imaging* 7(3), 564–574 (1997).

38 Gribbestad IS, Gjesdal KI, Nilsen G, Lundgren S, Hjelstuen MHB, Jackson A: An introduction to dynamic contrast-enhanced MRI in oncology. In: *Dynamic Contrast-Enhanced Magnetic Resonance Imaging in Oncology.* Jackson A, Bucklay DL, Parker GJM (Eds). Springer-Verlag, Germany 3–22 (2003).

39 Marquardt DW: An algorithm for least-squares estimation of nonlinear parameters. *J. Soc. Ind. Appl. Mathematics* 11(2), 431–441 (1963).

40 Nelder JA, Mead R: A simplex algorithm for function minimization. *Comput. J.* 7(4), 308–313 (1965).

41 Ahearn TS, Staff RT, Redpath TW, Semple SI: The use of the Levenberg–Marquardt curve-fitting algorithm in pharmacokinetic modeling of DCE-MRI data. *Phys. Med. Biol.* 50(9), N85–N92 (2005).

42 Tofts PS, Brix G, Buckley DL *et al.*: Estimating kinetic parameters from dynamic contrast-enhanced T_1-weighted MRI of a diffusable tracer: standardized quantities and symbols. *J. Magn. Reson. Imaging* 10(3), 223–232 (1999).

■■ Standardization of the terminology used in pharmacokinetic modeling. Many models are discussed and compared.

43 Weisskoff RM, Chesler D, Boxerman JL, Rosen BR: Pitfalls in MR measurement of tissue blood flow with intravascular tracers: which mean transit time? *Magn. Reson. Med.* 29(4), 553–558 (1993).

44 Brix G, Semmler W, Port R, Schad L, Layer G, Lorenz W: Pharmacokinetic parameters in CNS Gd-DTPA enhanced MR imaging. *J. Comput. Assist. Tomogr.* 15, 621–628 (1991).

45 Tofts PS, Kermode AG: Measurement of the blood–brain barrier permeability and leakage space using dynamic MR imaging. 1. Fundamental concepts. *Magn. Reson. Med.* 17(2), 357–367 (1991).

46 Larsson HB, Stubgaard M, Frederiksen JL, Jensen M, Henriksen O, Paulson OB: Quantitation of blood–brain barrier defect by magnetic resonance imaging and gadolinium-DTPA in patients with multiple sclerosis and brain tumors. *Magn. Reson. Med.* 16(1), 117–131 (1990).

47 St Lawrence KS, Lee TY: An adiabatic approximation to the tissue homogeneity model for water exchange in the brain: I. Theoretical derivation. *J. Cereb. Blood Flow Metab.* 18(12), 1365–1377 (1998).

48 Li KL, Zhu XP, Checkley DR *et al.*: Simultaneous mapping of blood volume and endothelial permeability surface area product in gliomas using iterative analysis of first-pass dynamic contrast enhanced MRI data. *Br. J. Radiol.* 76(901), 39–50 (2003).

49 Su MY, Jao JC, Nalcioglu O: Measurement of vascular volume fraction and blood–tissue permeability constants with a pharmacokinetic model: studies in rat muscle tumors with dynamic Gd-DTPA enhanced MRI. *Magn. Reson. Med.* 32(6), 714–724 (1994).

50 Li X, Rooney WD, Springer CS Jr: A unified magnetic resonance imaging pharmacokinetic theory: intravascular and extracellular contrast reagents. *Magn. Reson. Med.* 54(6), 1351–1359 (2005).

51 Li KL, Henry RG, Wilmes LJ *et al.*: Kinetic assessment of breast tumors using high spatial resolution signal enhancement ratio (SER) imaging. *Magn. Reson. Med.* 58(3), 572–581 (2007).

52 Ahearn TS, Staff RT, Redpath TW, Semple SI: The effects of renal variation upon measurements of perfusion and leakage volume in breast tumors. *Phys. Med. Biol.* 49(10), 2041–2051 (2004).

53 Walker-Samuel S, Leach MO, Collins DJ: Reference tissue quantification of DCE-MRI data without a contrast agent calibration. *Phys. Med. Biol.* 52(3), 589–601 (2007).

54 Yankeelov TE, Luci JJ, Lepage M *et al.*: Quantitative pharmacokinetic analysis of DCE-MRI data without an arterial input function: a reference region model. *Magn. Reson. Imaging* 23(4), 519–529 (2005).

55 Johnson G, Wetzel SG, Cha S, Babb J, Tofts PS: Measuring blood volume and vascular transfer constant from dynamic, T_2*-weighted contrast-enhanced MRI. *Magn. Reson. Med.* 51(5), 961–968 (2004).

56 Gruner R, Bjornara BT, Moen G, Taxt T: Magnetic resonance brain perfusion imaging with voxel-specific arterial input functions. *J. Magn. Reson. Imaging* 23(3), 273–284 (2006).

57 Parker GJ, Roberts C, Macdonald A *et al.*: Experimentally-derived functional form for a population-averaged high-temporal-resolution arterial input function for dynamic contrast-enhanced MRI. *Magn. Reson. Med.* 56(5), 993–1000 (2006).

58 Wang Y, Huang W, Panicek DM, Schwartz LH, Koutcher JA: Feasibility of using limited-population-based arterial input function for pharmacokinetic modeling of osteosarcoma dynamic contrast-enhanced MRI data. *Magn. Reson. Med.* 59(5), 1183–1189 (2008).

59 Zhang JL, Rusinek H, Bokacheva L, Chen Q, Storey P, Lee VS: Use of cardiac output to improve measurement of input function in quantitative dynamic contrast-enhanced MRI. *J. Magn. Reson. Imaging* 30(3), 656–665 (2009).

60 Azlan C, Di Giovanni P, Ahearn TS *et al.*: Assessment of errors in T_1 measurement used for quantitative DCE-MRI: consequences for pharmacokinetic modeling. *Proceedings of the*

17th Annual Meeting of the International Society for Magnetic Resonance in Medicine. Honolulu, Hawaii, USA, 18–24 April 2009.

61   Brookes JA, Redpath TW, Gilbert FJ, Murray AD, Staff RT: Accuracy of T_1 measurement in dynamic contrast-enhanced breast MRI using two and three dimensional variable flip angle fast low-angle shot. *J. Magn. Reson. Imaging* 9(2), 163–171 (1999).

62   Redpath T: Calibration of the Aberdeen NMR imager for proton spin-lattice relaxation time measurements *in vivo. Phys. Med. Biol.* 27, 1057–1065 (1982).

63   Azlan C, Di Giovanni P, Ahearn TS *et al.*: The effect of B1 inhomogeneity on enhancement ratio measurements using DCE-MRI of the breast at 3T. *Proceedings of the 17th Annual Meeting of the International Society for Magnetic Resonance in Medicine.* Honolulu, Hawaii, USA, 18–24 April 2009.

64   Kuhl CK, Kooijman H, Gieseke J, Schild HH: Effect of B1 inhomogeneity on breast MRI at 3.0 T. *Radiology* 244(3), 929–930 (2007).

■   **Highlights the importance of field homogeneity on imaging.**

65   Kuhl CK: MRI of breast tumors. *Eur. Radiol.* 10(1), 46–58 (2000).

66   Heywang-Kobrunner SH, Viehweg P, Heinig A, Kuchler C: Contrast-enhanced MRI of the breast: accuracy, value, controversies, solutions. *Eur. J. Radiol.* 24(2), 94–108 (1997).

67   Szabo BK, Aspelin P, Wiberg MK, Bone B: Dynamic MRI of the breast. Analysis of kinetic and morphologic diagnostic criteria. *Acta Radiol.* 44(4), 379–386 (2003).

68   Buadu LD, Murakami J, Murayama S *et al.*: Breast lesions: correlation of contrast medium enhancement patterns on MR images with histopathologic findings and tumor angiogenesis. *Radiology* 200, 639 (1996).

69   Kaiser WA, Zeitler E: MRI of the breast: fast imaging sequences with and without Gd-DTPA. Preliminary observations. *Radiology* 170(3 Pt 1), 681–686 (1989).

70   Gilles R, Guinebietier J, Lucidarme O *et al.*: Non-palpable breast tumors: diagnosis with contrast enhanced subtraction dynamic MR imaging. *Radiology* 191, 625–631 (1994).

71   Warren RM, Thompson D, Pointon LJ *et al.*: Evaluation of a prospective scoring system designed for a multicenter breast MRI screening study. *Radiology* 239(3), 677–685 (2006).

72   Hylton N: Dynamic contrast-enhanced magnetic resonance imaging as an imaging biomarker. *J. Clin. Oncol.* 24(20), 3293–3298 (2006).

73   Furuta A, Ishibashi T, Takahashi S *et al.*: Magnetic resonance imaging of breast cancer: correlation between contrast enhancement and tumor angiogenesis. *Nippon Igaku Hoshasen Gakkai Zasshi* 59(12), 682–688 (1999).

74   Radjenovic A, Dall BJ, Ridgway JP, Smith MA: Measurement of pharmacokinetic parameters in histologically graded invasive breast tumors using dynamic contrast-enhanced MRI. *Br. J. Radiol.* 81(962), 120–128 (2008).

75   Londero V, Bazzocchi M, Del Frate C *et al.*: Locally advanced breast cancer: comparison of mammography, sonography and MRI in evaluation of residual disease in women receiving neoadjuvant chemotherapy. *Eur. Radiol.* 14(8), 1371–1379 (2004).

76   Julius T, Kemp SE, Kneeshaw PJ, Chaturvedi A, Drew PJ, Turnbull LW: MRI and conservative treatment of locally advanced breast cancer. *Eur. J. Surg. Oncol.* 31(10), 1129–1134 (2005).

77   Blue Cross and Blue Shield Association. Magnetic resonance imaging of the breast for preoperative evaluation in patients with localized breast cancer. Volume 18, No. 8 (2004).

78   de Bazelaire C, Alsop DC, George D *et al.*: Magnetic resonance imaging-measured blood flow change after antiangiogenic therapy with PTK787/ZK 222584 correlates with clinical outcome in metastatic renal cell carcinoma. *Clin. Cancer Res.* 14(17), 5548–5554 (2008).

79   Blue Cross and Blue Shield Association. Breast MRI for management of patients with locally advanced breast cancer who are being referred for neoadjuvant chemotherapy. Volume 19, No. 7 (2004).

80   Chang YC, Huang CS, Liu YJ, Chen JH, Lu YS, Tseng WY: Angiogenic response of locally advanced breast cancer to neoadjuvant chemotherapy evaluated with parametric histogram from dynamic contrast-enhanced MRI. *Phys. Med. Biol.* 49(16), 3593–3602 (2004).

81   Ah-See ML, Makris A, Taylor NJ *et al.*: Early changes in functional dynamic magnetic resonance imaging predict for pathologic response to neoadjuvant chemotherapy in primary breast cancer. *Clin. Cancer Res.* 14(20), 6580–6589 (2008).

82   Rieber A, Brambs HJ, Gabelmann A, Heilmann V, Kreienberg R, Kuhn T: Breast MRI for monitoring response of primary breast cancer to neo-adjuvant chemotherapy. *Eur. Radiol.* 12(7), 1711–1719 (2002).

83   Martincich L, Montemurro F, De Rosa G *et al.*: Monitoring response to primary chemotherapy in breast cancer using dynamic

contrast-enhanced magnetic resonance imaging. *Breast Cancer Res. Treat.* 83(1), 67–76 (2004).

84   Pickles MD, Lowry M, Manton DJ, Gibbs P, Turnbull LW: Role of dynamic contrast enhanced MRI in monitoring early response of locally advanced breast cancer to neoadjuvant chemotherapy. *Breast Cancer Res. Treat.* 91(1), 1–10 (2005).

85   Padhani AR, Hayes C, Assersohn L *et al.*: Prediction of clinicopathologic response of breast cancer to primary chemotherapy at contrast-enhanced MR imaging: initial clinical results. *Radiology* 239(2), 361–374 (2006).

86   Yu HJ, Chen JH, Mehta RS, Nalcioglu O, Su MY: MRI measurements of tumor size and pharmacokinetic parameters as early predictors of response in breast cancer patients undergoing neoadjuvant anthracycline chemotherapy. *J. Magn. Reson. Imaging* 26(3), 615–623 (2007).

87   Manton DJ, Chaturvedi A, Hubbard A *et al.*: Neoadjuvant chemotherapy in breast cancer: early response prediction with quantitative MRI and spectroscopy. *Br. J. Cancer* 94(3), 427–435 (2006).

88   Rose PG, Bundy BN, Watkins EB *et al.*: Concurrent cisplatin-based radiotherapy and chemotherapy for locally advanced cervical cancer. *N. Engl. J. Med.* 340(15), 1144–1153 (1999).

89   Morris M, Eifel PJ, Lu J *et al.*: Pelvic radiation with concurrent chemotherapy compared with pelvic and para-aortic radiation for high-risk cervical cancer. *N. Engl. J. Med.* 340(15), 1137–1143 (1999).

90   Keys HM, Bundy BN, Stehman FB *et al.*: Cisplatin, radiation, and adjuvant hysterectomy compared with radiation and adjuvant hysterectomy for bulky stage IB cervical carcinoma. *N. Engl. J. Med.* 340(15), 1154–1161 (1999).

91   Souhami L, Seymour R, Roman TN *et al.*: Weekly cisplatin plus external beam radiotherapy and high dose rate brachytherapy in patients with locally advanced carcinoma of the cervix. *Int. J. Radiat. Oncol. Biol. Phys.* 27(4), 871–878 (1993).

92   Sala E, Wakely S, Senior E, Lomas D: MRI of malignant neoplasms of the uterine corpus and cervix. *Am. J. Roentgenol.* 188(6), 1577–1587 (2007).

93   Mayr NA, Yuh WT, Magnotta VA *et al.*: Tumor perfusion studies using fast magnetic resonance imaging technique in advanced cervical cancer: a new noninvasive predictive assay. *Int. J. Radiat. Oncol. Biol. Phys.* 36(3), 623–633 (1996).

94   Mayr NA, Yuh WT, Zheng J *et al.*: Prediction of tumor control in patients with cervical cancer: analysis of combined volume and dynamic enhancement pattern by MR imaging. *Am. J. Roentgenol.* 170(1), 177–182 (1998).

95   Hawighorst H, Knapstein PG, Weikel W *et al.*: Cervical carcinoma: comparison of standard and pharmacokinetic MR imaging. *Radiology* 201(2), 531–539 (1996).

96   Loncaster JA, Carrington BM, Sykes JR *et al.*: Prediction of radiotherapy outcome using dynamic contrast enhanced MRI of carcinoma of the cervix. *Int. J. Radiat. Oncol. Biol. Phys.* 54(3), 759–767 (2002).

97   Zahra M, Sala E, Lomas DJ *et al.*: The predictive role of functional imaging in cervix cancer. *Clin. Oncol.* 19(Suppl. 3), S51 (2007).

98   Semple SI, Staff RT, Heys SD *et al.*: Baseline MRI delivery characteristics predict change in invasive ductal breast carcinoma PET metabolism as a result of primary chemotherapy administration. *Ann. Oncol.* 17(9), 1393–1398 (2006).

99   Semple SI, Gilbert FJ, Redpath TW *et al.*: The relationship between vascular and metabolic characteristics of primary breast tumors. *Eur. Radiol.* 14(11), 2038–2045 (2004).

100   Semple SIK, Harry VN, Parkin DE, Gilbert FJ: A combined pharmacokinetic and radiological assessment of dynamic-contrast enhanced magnetic resonance imaging predicts response to chemoradiation in locally advanced cervical cancer. *Int. J. Radiat. Oncol. Biol. Phys.* (2009) (In Press).

101   Hurwitz H, Fehrenbacher L, Novotny W *et al.*: Bevacizumab plus irinotecan, fluorouracil, and leucovorin for metastatic colorectal cancer. *N. Engl. J. Med.* 350(23), 2335–2342 (2004).

102   Jain RK, Duda DG, Clark JW, Loeffler JS: Lessons from Phase III clinical trials on anti-VEGF therapy for cancer. *Nat. Clin. Pract. Oncol.* 3(1), 24–40 (2006).

103   Tuncbilek N, Karakas HM, Altaner S: Dynamic MRI in indirect estimation of microvessel density, histologic grade, and prognosis in colorectal adenocarcinomas. *Abdom. Imaging* 29(2), 166–172 (2004).

104   George ML, Dzik-Jurasz AS, Padhani AR *et al.*: Non-invasive methods of assessing angiogenesis and their value in predicting response to treatment in colorectal cancer. *Br. J. Surg.* 88(12), 1628–1636 (2001).

105   Moeller BJ, Cao Y, Li CY, Dewhirst MW: Radiation activates HIF-1 to regulate vascular radiosensitivity in tumors: role of reoxygenation, free radicals, and stress granules. *Cancer Cell* 5(5), 429–441 (2004).

106   de Vries A, Griebel J, Kremser C *et al.*: Monitoring of tumor microcirculation during fractionated radiation therapy in patients with rectal carcinoma: preliminary results and implications for therapy. *Radiology* 217(2), 385–391 (2000).

107   Devries AF, Griebel J, Kremser C *et al.*: Tumor microcirculation evaluated by dynamic magnetic resonance imaging predicts therapy outcome for primary rectal carcinoma. *Cancer Res.* 61(6), 2513–2516 (2001).

108   Yang JC, Haworth L, Sherry RM *et al.*: A randomized trial of bevacizumab, an anti-vascular endothelial growth factor antibody, for metastatic renal cancer. *N. Engl. J. Med.* 349(5), 427–434 (2003).

109   McCarthy M: Antiangiogenesis drug promising for metastatic colorectal cancer. *Lancet* 361(9373), 1959 (2003).

110   Wedam SB, Low JA, Yang SX *et al.*: Antiangiogenic and antitumor effects of bevacizumab in patients with inflammatory and locally advanced breast cancer. *J. Clin. Oncol.* 24(5), 769–777 (2006).

111   Reddick WE, Guo J, Qing J, McCarville ME, Daw NC: Preliminary experiences with 3D DCE-MRI evaluation of children treated for osteosarcoma with chemotherapy plus bevacizumab. *Proceedings of the 17th Annual Meeting of the International Society for Magnetic Resonance in Medicine.* Honolulu, Hawaii, USA, 18–24 April 2009.

112   Morgan B, Thomas AL, Drevs J *et al.*: Dynamic contrast-enhanced magnetic resonance imaging as a biomarker for the pharmacological response of PTK787/ZK 222584, an inhibitor of the vascular endothelial growth factor receptor tyrosine kinases, in patients with advanced colorectal cancer and liver metastases: results from two Phase I studies. *J. Clin. Oncol.* 21(21), 3955–3964 (2003).

113   Leach MO, Brindle KM, Evelhoch JL *et al.*: The assessment of antiangiogenic and antivascular therapies in early-stage clinical trials using magnetic resonance imaging: issues and recommendations. *Br. J. Cancer* 92(9), 1599–1610 (2005).

114   Tofts PS: Modeling tracer kinetics in dynamic Gd-DTPA MR imaging. *J. Magn. Reson. Imaging* 7(1), 91–101 (1997).

115   Brasch R, Pham C, Shames D *et al.*: Assessing tumor angiogenesis using macromolecular MRI contrast media. *J. Magn. Reson. Imaging* 7, 68–74 (1997).

116   Baxter AB, Melnikoff S, Stites DP, Brasch RC: AUR Memorial Award (1991). Immunogenicity of gadolinium-based contrast agents for magnetic resonance imaging. Induction and characterization of antibodies in animals. *Invest. Radiol.* 26(12), 1035–1040 (1991).

117   White DL, Wang S, Aicher K, Dupon J, Engelstad B, Brasch R: Albumin-(Gd-DTPA)15–20: whole body clearance, and organ distribution of gadolinium. *Proceedings of the 8th Annual Meeting of the Society of Magnetic Resonance Imaging in Medicine.* Amsterdam, The Netherlands, 12–18 August 1989.

118   Cyran CC, Fu Y, Raatschen HJ *et al.*: New macromolecular polymeric MRI contrast agents for application in the differentiation of cancer from benign soft tissues. *J. Magn. Reson. Imaging* 27(3), 581–589 (2008).

119   Barrett T, Kobayashi H, Brechbiel M, Choyke PL: Macromolecular MRI contrast agents for imaging tumor angiogenesis. *Eur. J. Radiol.* 60(3), 353–366 (2006).

120   Mohs AM, Lu ZR: Gadolinium(III)-based blood-pool contrast agents for magnetic resonance imaging: status and clinical potential. *Expert Opin. Drug Deliv.* 4(2), 149–164 (2007).

121   Digilio G, Catanzaro V, Fedeli F *et al.*: Targeting exofacial protein thiols with Gd(III) complexes. An efficient procedure for MRI cell labelling. *Chem. Comm.* 8, 893–895 (2009).

122   Strijkers GJ, Hak S, Kok MB, Springer CS Jr, Nicolay K: Three-compartment T_1 relaxation model for intracellular paramagnetic contrast agents. *Magn. Reson. Med.* 61(5), 1049–1058 (2009).

123   Zwick S, Strecker R, Kiselev V *et al.*: Assessment of vascular remodeling under antiangiogenic therapy using DCE-MRI and vessel size imaging. *J. Magn. Reson. Imaging* 29(5), 1125–1133 (2009).

124   Hassid Y, Furman-Haran E, Margalit R, Eilam R, Degani H: Noninvasive magnetic resonance imaging of transport and interstitial fluid pressure in ectopic human lung tumors. *Cancer Res.* 66(8), 4159–4166 (2006).

■ Websites

201   Quantitative Imaging Biomarkers Alliance (QIBA). http://qibawiki.rsna.org/index.php?title=Main_Page (Accessed 17 July 2009)

202   DCE-MRI Project Page. http://qibawiki.rsna.org/index.php?title=DCE-MRI. (Accessed 17 July 2009)